PUBLICATIONS OF THE ASTRONOMICAL SOCIETY OF THE PACIFIC, **124**:854–860, 2012 August

The Palomar Transient Factory photometric catalog 1.0

E. O. OFEK,[1] R. LAHER,[2] J. SURACE,[2] D. LEVITAN,[3] B. SESAR,[3] A. HORESH,[3] N. LAW,[4] J. C. VAN EYKEN,[5] S. R. KULKARNI,[3] T. A. PRINCE,[3] P. NUGENT,[6] M. SULLIVAN,[7] O. YARON,[1] A. PICKLES,[8] M. AGÜEROS,[9] I. ARCAVI,[1] L. BILDSTEN,[10,11] J. BLOOM,[12] S. B. CENKO,[12] A. GAL-YAM,[1] C. GRILLMAIR,[2] G. HELOU,[2] M. M. KASLIWAL,[1] D. POZNANSKI,[13] AND R. QUIMBY[14]

Received 2012 February 28; accepted 2012 June 05; published 2012 August 29

ABSTRACT. We constructed a photometrically calibrated catalog of non-variable sources from the Palomar Transient Factory (PTF) observations. The first version of this catalog presented here, the PTF photometric catalog 1.0, contains calibrated $R_{\rm PTF}$-filter magnitudes for $\approx 2.1 \times 10^7$ sources brighter than magnitude 19, over an area of $\approx 11,233$ deg^2. The magnitudes are provided in the PTF photometric system, and the color of a source is required in order to convert these magnitudes into other magnitude systems. We estimate that the magnitudes in this catalog have a typical accuracy of about 0.02 mag with respect to magnitudes from the Sloan Digital Sky Survey. The median repeatability of our catalog's magnitudes for stars between 15 and 16 mag, is about 0.01 mag and it is over 0.03 mag for 95% of the sources in this magnitude range. The main goal of this catalog is to provide reference magnitudes for photometric calibration of visible light observations. Subsequent versions of this catalog, which will be published incrementally online, will be extended to cover a larger sky area and will also include $g_{\rm PTF}$-filter magnitudes, as well as variability and proper-motion information.

Online material: color figures

1. INTRODUCTION

All-sky photometrically calibrated stellar catalogs are being used to measure the true apparent flux of astrophysical sources. Other approaches, such as observing standard stars (e.g., Landolt 1992), are time-consuming, since they require additional observations, that are not of the source of interest, under photometric conditions. Therefore, it is desirable to have an all-sky catalog that contains calibrated stellar magnitudes. To date, the most widely used catalog for this purpose is probably the USNO-B1.0 (Monet et al. 2003), which provides the blue, red, and near-infrared photographic plate magnitudes for about 10^9 sources. Unfortunately, the photometric measurements in the USNO-B1.0 catalog show significant systematic variations in the magnitude zero point as a function of the position on the sky ($\sim$0.5 mag), even at small angular scales (Sesar et al. 2006).

The Sloan Digital Sky Survey (SDSS; York et al. 2000) is calibrated to an accuracy of better than 2% (Adelman-McCarthy et al. 2008; Padmanabhan et al. 2008). However, SDSS Data Release 8 only covers about one-third of the celestial sphere. Another possibility is to use bright Tycho-2 (Høg et al. 2000) stars to photometrically calibrate images (Ofek 2008; Pickles & Depagne 2010). However, this approach requires that Tycho stars brighter than magnitude $\approx$12 are not saturated in the images.

The Palomar Transient Factory[15] (Law et al. 2009; Rau et al. 2009) is a synoptic survey designed to explore the transient sky and to study stellar variability. The project utilizes the 48″ Samuel Oschin Schmidt Telescope at Palomar Observatory.

[1] Benoziyo Center for Astrophysics, Weizmann Institute of Science, 76100 Rehovot, Israel.
[2] Spitzer Science Center, California Institute of Technology, Pasadena, CA 91125.
[3] Division of Physics, Mathematics and Astronomy, California Institute of Technology, Pasadena, CA 91125.
[4] Dunlap Institute for Astronomy and Astrophysics, University of Toronto, Toronto, ON M5S 3H4, Canada.
[5] NASA Exoplanet Science Institute, California Institute of Technology, Pasadena, CA 91125.
[6] Department of Astronomy, University of California, Berkeley, CA 94720-3411.
[7] Department of Physics, University of Oxford, Oxford OX1 3RH, UK.
[8] Las Cumbres Observatory Global Telescope Network, Santa Barbara, CA 93117.
[9] Department of Astronomy, Columbia University, New York, NY 10027.
[10] Department of Physics, Broida Hall, University of California, Santa Barbara, CA 93106.
[11] Kavli Institute for Theoretical Physics, Kohn Hall, University of California, Santa Barbara, CA 93106.
[12] Department of Astronomy, University of California, Berkeley, CA 94720-3411.
[13] School of Physics and Astronomy, Tel-Aviv University, Israel.
[14] Institute for the Physics and Mathematics of the Universe, University of Tokyo, Kashiwa-shi, Chiba, 277-8583, Japan.

[15] See http://www.astro.caltech.edu/ptf/.

The telescope has a digital camera equipped with 11 active CCDs,[16] each 2 K × 4 K pixels (Rahmer et al. 2008), and it has been surveying the northern sky since 2009 March. Each PTF image covers 7.26 deg^2 with a scale of 1.01″ pixel^{-1}. The median point-spread function full width at half-maximum is ≈2″ and is uniform over the camera field of view (Law et al. 2010). The PTF main survey is currently performed in the g band during dark time and in the Mould R band during bright time, but most of the data taken prior to 2011 January were obtained using the R-band filter. In addition, a few nights around times of full Moon are used for surveying the sky with narrow-band Hα filters. An overview of the PTF survey and its first-year performance is given in Law et al. (2010).

The PTF data are reduced by pipelines running at California Institute of Technology's Infrared Processing and Analysis Center (IPAC), and the processing includes astrometric and photometric calibration. Here, we build on the PTF photometric calibration to construct a catalog of calibrated nonvariable sources. This catalog can be used to photometrically calibrate other visible-light observations.

This article is organized as follows: in § 2, we briefly discuss the PTF photometric calibration; the construction of the photometric catalog is described in § 3; the catalog is presented in § 4; we discuss accuracy and repeatability in § 5; and finally, we conclude in § 6.

2. BRIEF DESCRIPTION OF THE PTF PHOTOMETRIC CALIBRATION

Here, we summarize the photometric calibration of PTF images, which is fundamental to the construction of the PTF photometric catalog. A full description can be found in Ofek et al. (2012).

We used images reduced by the IPAC-PTF pipeline (Grillmair et al. 2010; Laher et al. 2012, in preparation). The processing includes splitting the multiextension FITS images, debiasing, flat-fielding, astrometric calibration, generation of mask images, source extraction, and photometric calibration. The astrometric calibration is performed relative to SDSS when possible and the UCAC-3 catalog (Zacharias et al. 2010) when SDSS information is not available. If a UCAC-3 solution is not found, then the astrometry is solved against USNO-B1.0 (Monet et al. 2003). The median astrometric rms in single axis is 0.11″, 0.13″, and 0.4″ for the SDSS, UCAC-3, and USNO-B1.0 catalogs, respectively. The masks flag pixels with image artifacts, including ghosts, halos, aircraft/satellite tracks, saturation, CCD bleeding, and dead/bad pixels. Sources that contain masked pixels inherit the pixels' flag and these are stored in the catalogs associated with the processed images.

Our photometric calibration method is similar to the classical method of observing standard stars through various air masses and assuming photometric conditions—i.e., the atmospheric transmission properties are constant in time and are a continuous function of air mass. On average, we typically observe ∼10^5 SDSS stars with a high signal-to-noise ratio (S/N) per CCD per night. Therefore, we usually have a sufficient number of photometric measurements to robustly constrain all calibration parameters for a given night.

After selecting high-S/N sources, we fit the difference between the instrumental magnitude measured in the PTF system (e.g., $R_{\rm PTF}^{\rm inst}$) and the standard star magnitudes measured by SDSS (e.g., $R_{\rm SDSS}$) with a simple model. The free parameters in this model include the global zero point of the image, color term, extinction coefficient, color/air-mass term, variation of the global zero point during the night, exposure time, and illumination correction. Here, the illumination correction represents variation of the photometric zero point as a function of position on the CCD. The latter correction is represented by two methods relative to the center of each CCD, which are described in Ofek et al. (2012). To generate the first version of the PTF photometric catalog, we used the model in which the variation of the photometric zero point with CCD position is a two-dimensional, low-order polynomial in the position across each CCD (i.e., eq. [3] in Ofek et al. (2012). The goodness of the fit is described by several estimators, including the rms of residuals of bright stars from the best-fit model (parameter APBSRMS in Table 2 in Ofek et al. (2012).

We note that the magnitudes produced by our calibration process are related to the SDSS magnitude system (and other systems) via the aforementioned color terms. In the case where the $r-i$ color of an object is known, it is possible to convert the PTF R-band magnitudes to other systems. These transformations are described in equations (4)–(7) in Ofek et al. (2012, while the color terms for the 11 active CCDs are given in Table 3 in Ofek et al. (2012. For reference, we present the PTF R-band filter transmission in Figure 1 and in Table 1. Subsequent

TABLE 1

PTF R-BAND FILTER TRANSMISSION

λ (Å)	Filter	QE_{std}	QE_{hr}	Atm.	Sys_{std}	Sys_{hr}
5,680.0	0.00	0.66	0.74	0.84	0.00	0.00
5,685.0	0.00	0.66	0.74	0.84	0.00	0.00
5,690.0	0.01	0.66	0.74	0.84	0.01	0.01
5,695.0	0.01	0.66	0.75	0.84	0.01	0.01
5,700.0	0.01	0.67	0.75	0.84	0.01	0.01

NOTE.—PTF R-band filter transmission (see also Fig. 1). λ is the wavelength, Filter is the filter transmission, QE is the CCD efficiency, Atm. is the atmosphere transmission calculated using a standard smooth atmosphere (Hayes & Latham 1975) for 1.7 km elevation and air mass 1.3, and Sys is the total efficiency calculated by multiplying the filter, QE and atmosphere transmissions. Subscript std stands for standard CCD, and hr stands for high resistivity (see Fig. 1 caption). Table 1 is shown in its entirety in the electronic edition of *PASP*. A portion is shown here regarding its form and content.

[16] The camera has 12 CCDs, one of which is not functional.

TABLE 2
RANGES OF PARAMETERS OF GOOD DATA

Parameter	CCDID	Min	Max	Units
Seeing	All	...	4.0	arcsec
MoonESB	All	−3.0	...	mag arcsec^{-2}
APBSRMS	All	...	0.04	mag
$\alpha_{c,R}$	0	0.190	0.244	mag mag^{-1}
$\alpha_{a,R}$	0	−0.182	−0.044	mag airmass^{-1}
$\alpha_{c,R}$	1	0.175	0.235	mag mag^{-1}
$\alpha_{a,R}$	1	−0.177	−0.039	mag airmass^{-1}
$\alpha_{c,R}$	2	0.178	0.226	mag mag^{-1}
$\alpha_{a,R}$	2	−0.187	−0.037	mag airmass^{-1}
$\alpha_{c,R}$	4	0.189	0.249	mag mag^{-1}
$\alpha_{a,R}$	4	−0.200	−0.038	mag airmass^{-1}
$\alpha_{c,R}$	5	0.200	0.254	mag mag^{-1}
$\alpha_{a,R}$	5	−0.198	−0.036	mag airmass^{-1}
$\alpha_{c,R}$	6	0.201	0.249	mag mag^{-1}
$\alpha_{a,R}$	6	−0.183	−0.027	mag airmass^{-1}
$\alpha_{c,R}$	7	0.172	0.238	mag mag^{-1}
$\alpha_{a,R}$	7	−0.177	−0.033	mag airmass^{-1}
$\alpha_{c,R}$	8	0.181	0.229	mag mag^{-1}
$\alpha_{a,R}$	8	−0.175	−0.049	mag airmass^{-1}
$\alpha_{c,R}$	9	0.165	0.237	mag mag^{-1}
$\alpha_{a,R}$	9	−0.188	−0.038	mag airmass^{-1}
$\alpha_{c,R}$	10	0.176	0.260	mag mag^{-1}
$\alpha_{a,R}$	10	−0.188	−0.038	mag airmass^{-1}
$\alpha_{c,R}$	11	0.188	0.248	mag mag^{-1}
$\alpha_{a,R}$	11	−0.189	−0.039	mag airmass^{-1}

NOTE.—Min and Max specify the range minimum and maximum, respectively. See text for details.

versions of the PTF photometric catalog will include $g_{\rm PTF}$ magnitudes, which will enable straightforward transformation into other magnitude systems.

3. CATALOG CONSTRUCTION

Version 1.0 of the catalog was constructed from PTF data taken before 2011 November, using the IPAC-PTF pipeline software version identifier (SVID) > 47. For this version of the catalog, we only used PTF fields that were observed with the Mould R band on at least three photometric nights under good conditions. The terms "photometric nights" and "good conditions" are not well defined and depend on the required photometric accuracy, and we selected images that had photometric and quality parameters within the ranges specified in Table 2.

A detailed description of the photometric parameters (i.e., APBSRMS, $\alpha_{c,R}$, and $\alpha_{a,R}$) and their distributions is available later in this article. Here, the MoonESB is the theoretical V-band excess in sky surface magnitude (negative number) due to the Moon, and this excess is calculated using the algorithm of Krisciunas & Schaefer (1991). APBSRMS is the root mean square of bright stars of the nightly photometric calibration residuals from the best fit, $\alpha_{c,R}$ is the R-band $r-i$ color-term coefficient of the nightly photometric solution, and $\alpha_{a,R}$ is the nightly R-band extinction coefficient. The allowed ranges of these parameters (listed in Table 2) correspond to ± 3 times the one standard deviation[17] from the median value of each parameter over all data taken with a given CCD.[18]

We choose PTF fields[19] that have at least three images taken on three different nights and which meet the criteria listed in Table 2. The requirement to analyze only images that were observed on three or more photometric nights is important in order to remove outliers that may be present in the data. For example, if a night was photometric for 90% of the time (e.g., clouds entered toward the end of the night), then our pipeline might claim that the night was photometric, but the calibration of some of the data would be poor. Therefore, in order to obtain the calibrated source magnitudes, it is important to average the data taken over several photometric nights. Moreover, observations taken on multiple nights allow us to calculate variability and proper-motion indicators.

To expedite processing in cases where we have more than 30 images of the same field, we truncated the number of images according to the following scheme: if more than 30 images of the same field taken on less than 30 unique nights were available, then we selected a single random image from each night. If more than 30 images taken on more than 30 unique nights were available, then we selected the 30 nights with the smallest APBSRMS parameter and chose one image from each one of these nights. Histograms of the number of unique nights and number of unique observations per object in the catalog are shown in Figure 2.

For each set of selected images of a given PTFFIELD/CCDID, we matched the sources in all of the images against a reference image with a matching radius of 1.5″. Here, the reference image was selected as the image of the field with the largest number of sources.[20] We note that in future catalog versions, we intend to use a deep co-add image for each PTFFIELD/CCDID as a reference image.

Next, we removed all the measurements that were masked by one of the following flags: source is deblended by SExtractor (Bertin & Arnouts 1996), aircraft/satellite track, high dark current, noisy/hot pixel, containing possible optical ghost, CCD-bleed, radiation hit,[21] saturated pixels, dead pixel, not a number, halo around bright star, and dirt on optics. These flags are described in detail in Laher et al. (2012, in preparation). The remaining photometric measurements are used to calculate the

[17] We used the sixty-eighth percentile divided by 2 as a robust estimator for one standard deviation.

[18] The CCD number is designated by CCDID, which ranges from 0 to 11 (CCDID = 3 is inoperable).

[19] A PTF field, denoted by PTFFIELD, is uniquely associated with a predefined sky position.

[20] Typically, this is the image with the best limiting magnitude.

[21] The current radiation hit/CCD bleed flag in the version of the PTF IPAC pipeline used here is not a good indicator for radiation hits.

TABLE 3
PTF Photometric Catalog 1.0

α_{J2000} (deg)	δ_{J2000} (deg)	N_{obs}	N_{night}	BestRMS (mag)	R_{PTF} (mag)	ΔR_{PTF} (mag)	$\Delta_- R_{PTF}$ (mag)	$\Delta_+ R_{PTF}$ (mag)	μ_{type} (mag)	$\Delta\mu_{type}$ (mag)	PTFFIELD	CCDID	Flag
42.532500	−31.087161	23	12	0.022	16.152	0.021	0.017	0.026	0.058	0.095	100111	09	1
42.786188	−31.086008	21	12	0.022	17.172	0.030	0.022	0.037	0.058	0.060	100111	09	1
42.593730	−31.085419	22	12	0.022	18.507	0.063	0.055	0.071	0.106	0.106	100111	09	1
42.525416	−31.081556	23	12	0.022	14.225	0.015	0.017	0.014	0.046	0.072	100111	09	1
42.953363	−31.080395	23	12	0.022	15.286	0.025	0.029	0.022	0.003	0.063	100111	09	1

Note.—Table is sorted by declination. See text for column descriptions. Table 3 is shown in its entirety at http://irsa.ipac.caltech.edu/ and on the Vizier Online Data Catalog at http://vizier.u-strasbg.fr/viz-bin/VizieR. A portion is shown here regarding its form and content.

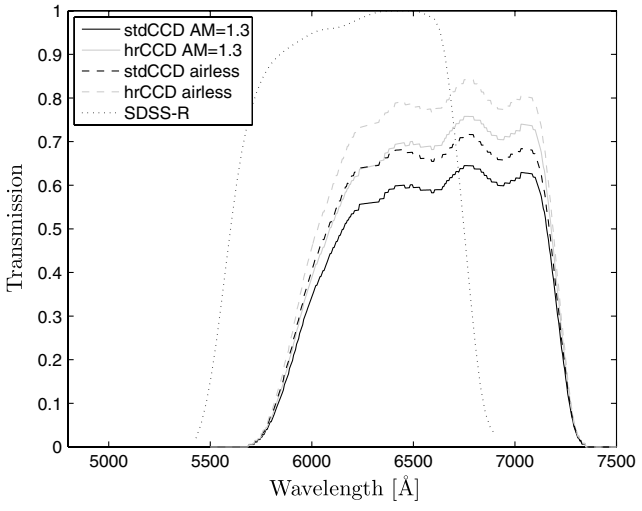

FIG. 1.—PTF R-band filter transmission at air mass of 1.3 (*solid line*) and no atmosphere (*dashed line*). The transmission is shown for the two CCD types in the PTF camera. std stands for the standard CCD (black line; CCDID 0,1,2,6,7,8,9,10,11) while hr stands for the high-resistivity CCDs (gray line; CCDID 4,5). The transmission was calculated by multiplying the filter, CCD and atmospheric transmissions. The atmospheric transmission was calculated using a standard smooth atmosphere (Hayes & Latham1975) for 1.7 km elevation and air mass 1.3. For reference we also show the transmission of the SDSS R-band filter.

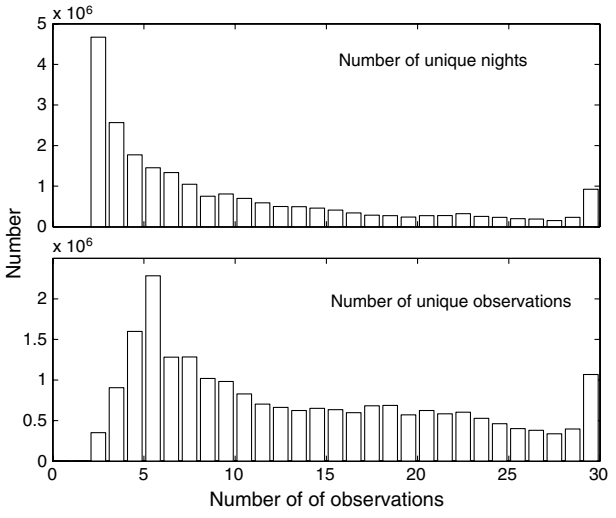

FIG. 2.—Histogram of the number of unique nights (*top*) and number of unique observations (*bottom*) per object in the catalog. The histogram of the number of unique observations peaks at six observations, twice of the value at which the histogram of number of unique night peaks. This reflects the fact that we obtained two observations per night for most fields until 2012 March.

mean photometric properties of each source in PTF photometric catalog 1.0.

Some of the PTF fields overlap in areal coverage. Therefore, some of the sources generated by the process described above are duplicates. We removed duplicate sources and kept the catalog entry that corresponded to the lowest PTFFIELD. We also removed all sources fainter than 19 mag. Sources fainter than ~19 mag have photometric errors that are larger than the photometric accuracy of this catalog.

4. THE CATALOG

The PTF photometric catalog is presented in Table 3. The catalog is also available online from the IPAC World Wide Web site[22] and the Vizier service.[23] The following columns are available:

$\alpha_{\rm J2000}$.—Median J2000.0 right ascension over all the images used to derive the photometry.

$\delta_{\rm J2000}$.—Median J2000.0 declination over all the images used to derive the photometry.

$N_{\rm obs}$.—Number of images that were used to derive the photometry.

$N_{\rm night}$.—Number of individual nights in which the images were taken.

BestRMS.—Best bright-star rms value (APBSRMS parameter) over all nights used.

$R_{\rm PTF}$.—Median R-band magnitude in the PTF system (i.e., not color-corrected to SDSS) over all epochs.

$\Delta R_{\rm PTF}$.—Error on the median R-band magnitude as calculated from the range containing 68% of the measurements divided by 2 (i.e., $[\Delta_{-}R_{\rm PTF} + \Delta_{+}R_{\rm PTF}]/2$).

$\Delta_{-}R_{\rm PTF}$.—Lower-bound error on the median R-band magnitude as calculated from the range between the median magnitude and the lower 16-percentile magnitude.

$\Delta_{+}R_{\rm PTF}$.—Upper-bound error on the median R-band magnitude as calculated from the range between the median magnitude and the upper 16-percentile magnitude. By construction,

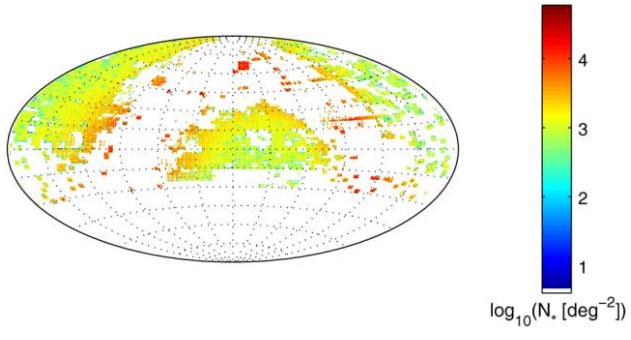

FIG. 3.—Coverage of the PTF photometric catalog 1.0 shown in an equal-area Aitoff projection in equatorial coordinates. RA $= 0^{\circ}$,Dec $= 0^{\circ}$ is in the center of the map. The coding shows the number of stars per deg^2 as calculated in a grid of 0.5×0.5 deg^2 cells on the sky. See the electronic edition of the *PASP* for a color version of this figure.

[22] See http://irsa.ipac.caltech.edu/.

[23] Vizier Online Data Catalog, http://vizier.u-strasbg.fr/viz-bin/VizieR.

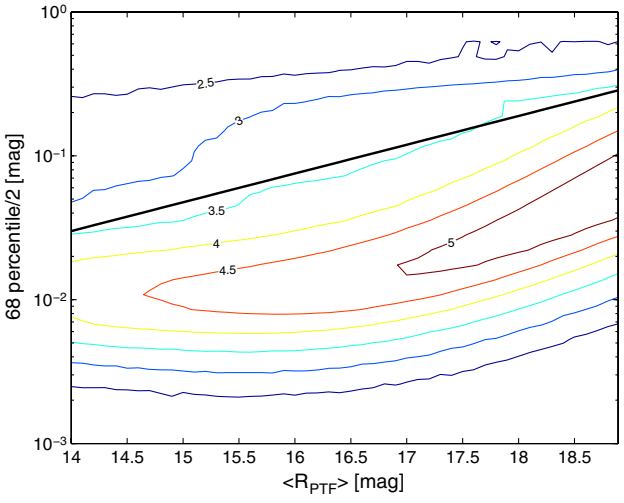

FIG. 4.—The 68-percentile range of the calibrated magnitude measurements divided by 2 as a function of the median magnitude of each star in the catalog. The contours indicate the $\log_{10}$ of the density of stars in this plane as calculated in cells of 0.1 mag in the X-axis and 0.1 dex in the Y-axis. The thick black line shows the error threshold we used to select photometric calibrators (i.e., Flag in Table 3). The figure demonstrates that the typical calibration error for bright stars is about 1%–2% and that the errors increase to about 0.06 mag for magnitude ~19. We note that while the 1% error at the bright end is mostly systematic, the ≈6% error at the faint end is mostly statistical (Poisson errors). About 2.6% of the stars are found above the solid line (i.e., stars with Flag = 0, which are not listed in the current version of the catalog). It is likely that a large fraction of the stars above the solid line are variable stars. See the electronic edition of the *PASP* for a color version of this figure.

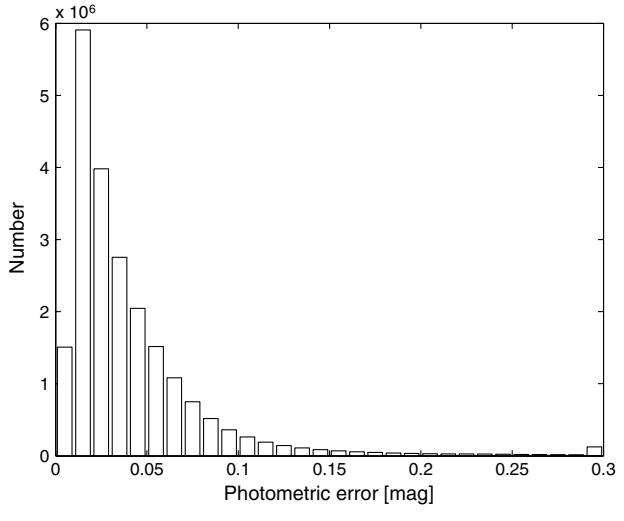

FIG. 5.—Histogram of the 68-percentile range divided by 2 (robust errors) distribution of all the stars in the PTF photometric catalog. The bins show the number of stars per 0.01 mag bins.

the sum of $\Delta_- R_{\rm PTF}$ and $\Delta_+ R_{\rm PTF}$ gives the 68-percentile range, and it is therefore an estimator for twice the 1-σ error.

$\mu_{\rm type}$.—Indicator that can be used to estimate if the source is resolved (e.g., galaxy) or unresolved (e.g., star). This is based on the SExtractor parameters MAG_AUTO-MU_MAX. MU_MAX measures the object surface magnitude in the object's central pixel. The parameter is normalized such that the median of $\mu_{\rm type}$ over the population of sources in the image is zero. Since most sources in PTF images are unresolved (stellarlike), this parameter has a value near zero for unresolved sources and extended sources will have negative $\mu_{\rm type}$ values. Based on our preliminary calibration, there is a ~2% probability that objects with $\mu_{\rm type} < -0.2$ are unresolved (stellar).

$\Delta\mu_{\rm type}$.—Standard deviation of the $\mu_{\rm type}$ as measured over all images used in the processing.

PTFFIELD.—PTF unique field identifier.

CCDID.—PTF CCD identifier (0 to 11).

Flag.—Flag that is set to 1 if the 68-percentile range is divided by 2 (i.e., $[\Delta_- R_{\rm PTF} + \Delta_+ R_{\rm PTF}]/2$) is smaller than $0.03 \times 10^{-0.2(14-R_{\rm PTF})}$ and is set to 0 otherwise. This flag can be useful in selecting sources for which the photometry is reliable and which are likely not strongly variable sources. In the current version of the catalog, we only list sources with Flag = 1.

The current catalog covers $11,233$ deg^2 and its sky coverage is shown in Figure 3. About $7,978$ deg^2 are found within the

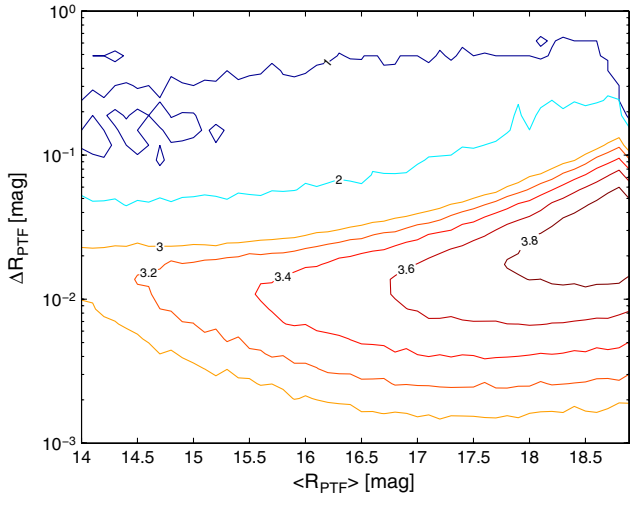

FIG. 6.—The differences between the duplicate measurements of the same stars taken on different fields or CCDs as a function of their mean magnitude. This plot is based on about 2.1×10^6 duplicate measurements. The contours indicate the $\log_{10}$ of the density of stars in this plane as calculated in cells of 0.1 mag in the X-axis and 0.1 dex in the Y-axis. The figure demonstrates that the typical repeatability of the photometric catalog is about 1%–2% at the bright end and 3% at the faint end and that in some cases repeatability of a few millimagnitudes is achieved even without applying relative photometry techniques (also see Fig. 4). See the electronic edition of the *PASP* for a color version of this figure.

footprint of SDSS-DR8, while $3,255$ deg^2 are outside the footprint of SDSS-DR8.

5. ACCURACY AND REPEATABILITY

Figure 4 gives contours of object density in the magnitude-scatter plane, where scatter is the 68 percentile range of the calibrated magnitude measurements divided by 2. The thick, solid black line shows the error threshold we used to select photometric calibrators (i.e., Flag $= 1$ in Table 3). Figure 5 presents the distribution of the 68-percentile range divided by 2 of all the stars in the PTF photometric catalog. This histogram suggest that 23.6% (4.3%) of the objects in the catalog have errors worse than 5% (10%). We note that fainter objects have larger photometric (Poisson) errors. Therefore, these errors do not represent the floor of systematic errors that can be achieved by using bright stars or many faint stars.

As discussed in § 4, some of the sources have duplicate measurements on different PTF fields and/or CCDs. Such duplicate measurements can be used to test the repeatability of the catalog over multiple CCDs. Figure 6 shows the differences between all 2.1×10^6 duplicate pairs as a function of their mean magnitude. We note that the mean difference between two data points generated from a Gaussian distribution is equal to 1.13 times the standard deviation of the Gaussian distribution. This figure suggests that our photometric calibration does not depend on the CCD in the camera from which the data were obtained. In the magnitude range of 15 to 16, the median repeatability is about 0.01 mag and 95% of the sources have a repeatability better than about 0.03 mag.

6. CONCLUSIONS

To summarize, we present a catalog of calibrated PTF R-band magnitudes of sources extracted from PTF images. The catalog covers about 28% of the celestial sphere, some of it outside the SDSS footprint. Conversion of PTF R-band magnitude to other magnitude systems requires knowledge of the source's color. We note that the scatter in colors of some populations of objects is small enough (e.g., RR Lyrae stars, asteroids) that their mean color can be used for conversion. Note that the current version of the catalog is designed as a photometric catalog rather than an astrometric catalog.

Future versions of this catalog will also provide the g-band magnitudes, which will allow one to apply color corrections directly with no assumptions. We also plan to include more robust variability information, source morphology and proper-motion measurements of individual sources.

We thank an anonymous referee for constructive comments. This article is based on observations obtained with the Samuel Oschin Telescope as part of the Palomar Transient Factory project, a scientific collaboration between the California Institute of Technology, Columbia University, Las Cumbres Observatory, the Lawrence Berkeley National Laboratory, the National Energy Research Scientific Computing Center, the University of Oxford, and the Weizmann Institute of Science. E. O. O. is the incumbent of the Arye Dissentshik career development chair and is grateful for support via a grant from the Israeli Ministry of Science, and the Helen Kimmel Center for Planetary Science. S. R. K. and his group are partially supported by NSF grant AST-0507734.

REFERENCES

Adelman-McCarthy, J. K., et al. 2008, ApJS, 175, 297
Bertin, E., & Arnouts, S. 1996, A&AS, 117, 393
Grillmair, C. J., et al. 2010, in ASP Conf. Ser. 434, Astronomical Data Analysis Software and Systems XIX (San Francisco: ASP), 28
Hayes, D. S., & Latham, D. W. 1975, ApJ, 197, 593
Høg, E., et al. 2000, A&A, 355, L 27
Krisciunas, K., & Schaefer, B. E. 1991, PASP, 103, 1033
Landolt, A. U. 1992, AJ, 104, 340
Law, N. M., et al. 2009, PASP, 121, 1395
———. 2010, Proc. SPIE, 7735, 77353M
Monet, D. G., et al. 2003, AJ, 125, 984
Ofek, E. O. 2008, PASP, 120, 1128
Ofek, E. O., Laher, R., Law, N., et al. 2012, PASP, 124, 62
Padmanabhan, N., et al. 2008, ApJ, 674, 1217
Pickles, A., & Depagne, É. 2010, PASP, 122, 1437
Rahmer, G., Smith, R., Velur, V., Hale, D., Law, N., Bui, K., Petrie, H., & Dekany, R. 2008, Proc. SPIE, 7014, 70144Y
Rau, A., et al. 2009, PASP, 121, 1334
Sesar, B., Svilković, D., & Ivezić, Ž., et al. 2006, AJ, 131, 2801
York, D. G., et al. 2000, AJ, 120, 1579
Zacharias, N., Finch, C., Girard, T., et al. 2010, AJ, 139, 2184